Overexpression of mitogen-activated protein kinase phosphatase-1 in endothelial cells reduces blood-brain barrier injury in a mouse model of ischemic stroke

Xiu-De Qin[1], Tai-Qin Yang[1], Jing-Hui Zeng[2], Hao-Bin Cai[1], Shao-Hua Qi[3], Jian-Jun Jiang[4], Ying Cheng[2], Long-Sheng Xu[5,*], Fan Bu[1,*]

https://doi.org/10.4103/1673-5374.363836

Date of submission: June 23, 2022

Date of decision: September 23, 2022

Date of acceptance: November 19, 2022

Date of web publication: January 5, 2023

From the Contents

Introduction	1743
Methods	1744
Results	1745
Discussion	1747

Graphical Abstract

Targeting mitogen-activated protein kinase phosphatase-1 (MKP-1) within endothelial cells may offer a potential therapeutic strategy for the treatment of ischemic stroke

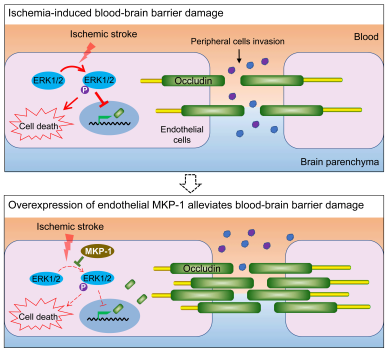

Abstract

Ischemic stroke can cause blood-brain barrier (BBB) injury, which worsens brain damage induced by stroke. Abnormal expression of tight junction proteins in endothelial cells (ECs) can increase intracellular space and BBB leakage. Selective inhibition of mitogen-activated protein kinase, the negative regulatory substrate of mitogen-activated protein kinase phosphatase (MKP)-1, improves tight junction protein function in ECs, and genetic deletion of MKP-1 aggravates ischemic brain injury. However, whether the latter affects BBB integrity, and the cell type-specific mechanism underlying this process, remain unclear. In this study, we established an adult male mouse model of ischemic stroke by occluding the middle cerebral artery for 60 minutes and overexpressed MKP-1 in ECs on the injured side via lentiviral transfection before stroke. We found that overexpression of MKP-1 in ECs reduced infarct volume, reduced the level of inflammatory factors interleukin-1β, interleukin-6, and chemokine C-C motif ligand-2, inhibited vascular injury, and promoted the recovery of sensorimotor and memory/cognitive function. Overexpression of MKP-1 in ECs also inhibited the activation of cerebral ischemia-induced extracellular signal-regulated kinase (ERK) 1/2 and the downregulation of occludin expression. Finally, to investigate the mechanism by which MKP-1 exerted these functions in ECs, we established an ischemic stroke model *in vitro* by depriving the primary endothelial cell of oxygen and glucose, and pharmacologically inhibited the activity of MKP-1 and ERK1/2. Our findings suggest that MKP-1 inhibition aggravates oxygen and glucose deprivation-induced cell death, cell monolayer leakage, and downregulation of occludin expression, and that inhibiting ERK1/2 can reverse these effects. In addition, co-inhibition of MKP-1 and ERK1/2 exhibited similar effects to inhibition of ERK1/2. These findings suggest that overexpression of MKP-1 in ECs can prevent ischemia-induced occludin downregulation and cell death via deactivating ERK1/2, thereby protecting the integrity of BBB, alleviating brain injury, and improving post-stroke prognosis.

Key Words: blood-brain barrier; brain injury; cerebral ischemia; endothelial cells; extracellular signal-regulated kinase 1/2; functional recovery; mitogen-activated protein kinase phosphatase 1; occludin; oxygen and glucose deprivation; transient middle cerebral artery occlusion

Introduction

Ischemic stroke is a sudden interruption of continuous blood flow to the brain, and is a primary cause of death and disability worldwide. One hallmark of ischemic stroke pathology is blood-brain barrier (BBB) breakdown, which is characterized by the death of brain capillary endothelial cells (ECs) and the disassembly of intercellular tight junction (TJ) proteins (Daneman, 2012; Cao et al., 2021; Deng et al., 2022). BBB hyperpermeability has been shown to increase the risk of tissue swelling and hemorrhage (Kimura and Harashima, 2022). In addition, circulating immune cells may penetrate the brain parenchyma, attracted by pro-inflammatory mediators produced by the injured tissue, which results in secondary injury and consequently worsens neurological outcomes (Jiang et al., 2018; Kim and Cho, 2021). However, the pathological mechanism of endothelium dysfunction in ischemic stroke remains unclear, and there is no effective therapeutic strategy for protecting BBB integrity.

Mitogen-activated protein kinase phosphatases (MKPs) are dual-specificity protein phosphatases that directly inactivate their mitogen-activated protein kinase (MAPK) substrates, primarily extracellular signal-regulated protein kinase (ERK) 1/2, P38, and Jun N-terminal kinase, by dephosphorylating threonine and tyrosine residues (Farooq and Zhou, 2004; Murphy and Blenis, 2006). MKP-1 was the first MKP to be discovered and is widely expressed in multiple cell types within the central nervous system, e.g., neurons, microglia, and ECs (Zakkar et al., 2008; Horita et al., 2010; Liu et al., 2014). MKP-1 has been implicated in the pathogenesis and development of various neurological diseases (Collins et al., 2015), including cerebral stroke. For example, depletion or pharmacological inhibition of MKP-1 worsens ischemic brain

[1]Department of Neurology & Psychology, Shenzhen Traditional Chinese Medicine Hospital, The Fourth Clinical Medical College of Guangzhou University of Chinese Medicine, Shenzhen, Guangdong Province, China; [2]Department of Cardiothoracic Surgery, Shenzhen Traditional Chinese Medicine Hospital, The Fourth Clinical Medical College of Guangzhou University of Chinese Medicine, Shenzhen, Guangdong Province, China; [3]Department of Neurology, The University of Texas Health Science Center at Houston, Houston, TX, USA; [4]Department of Nephrology, Shenzhen Traditional Chinese Medicine Hospital, The Fourth Clinical Medical College of Guangzhou University of Chinese Medicine, Shenzhen, Guangdong Province, China; [5]Department of Anesthesiology and Pain Medicine, The Affiliated Hospital of Jiaxing University, Jiaxing, Zhejiang Province, China

*Correspondence to: Fan Bu, PhD, fanbu123@outlook.com; Long-Sheng Xu, MS, xlsh2468@163.com.

https://orcid.org/0000-0002-0051-6037 (Fan Bu); https://orcid.org/0000-0002-6091-6323 (Long-Sheng Xu)

Funding: *This study was supported by Research Start-up Funding of Shenzhen Traditional Chinese Medicine Hospital, No. 2021-07 (to FB), Sanming Project of Medicine in Shenzhen, No. SZZYSM 202111011 (to XDQ and FB), Key Discipline Established by Zhejiang Province, Jiaxing City Jointly-Pain Medicine, No. 2019-ss-ttyx (to LSX), and Jiaxing Key Laboratory of Neurology and Pain Medicine, No. [2014]81 (to LSX).*

How to cite this article: *Qin XD, Yang TQ, Zeng JH, Cai HB, Qi SH, Jiang JJ, Cheng Y, Xu LS, Bu F (2023) Overexpression of mitogen-activated protein kinase phosphatase-1 in endothelial cells reduces blood-brain barrier injury in a mouse model of ischemic stroke. Neural Regen Res 18(8):1743-1749.*

injury (Liu et al., 2014), in contrast to the generally beneficial effect of ERK1/2 and P38 inhibitors in animal models of hemorrhagic and ischemic stroke (Sun and Nan, 2016). Liu et al. (2014) suggested that MKP-1 may protect against ischemic brain injury in a cell type-specific manner. They found that MKP-1 possesses anti-apoptotic and anti-inflammatory properties by controlling the activity of microglial P38 in the mouse brain. In the hemorrhagic stroke model, subarachnoid hemorrhage induces phosphorylation-mediated activation of ERK1/2 within the endothelium, as well as marked upregulation of matrix metallopeptidase 9, a key factor causing BBB damage and further expansion of brain injury (Parker et al., 2013). Blocking the ERK pathway prevents upregulation of matrix metallopeptidase 9 and activation of the cerebrovascular inflammatory response (Maddahi et al., 2012), suggesting that inhibiting MAPKs signaling in ECs could help prevent stroke-induced BBB disruption.

Alterations in TJs are a main cause of increased BBB permeability. The TJs occludin, claudin-5, and zonula occludens 1 are well studied. Their stepwise modification, translocation, and degradation take place from hours to days after ischemia, which determines the severity of BBB disruption and brain injury (González-Mariscal et al., 2008; Rodrigues and Granger, 2015; Zhang et al., 2021). MAPKs can hamper vascular barrier integrity by disrupting intercellular junctions in a multitude of diseases. For instance, cell cytotoxicity induced by oxygen and glucose deprivation (OGD) is prevented by inhibition of ERK1/2 signaling in cultured ECs from mice (Narasimhan et al., 2009). Excess salt exacerbates BBB leakage via P38-dependent down-regulation of TJ proteins, including occludin and zonula occludens 1, as demonstrated by *in vivo* and *in vitro* ischemic models (Zhang et al., 2015). Furthermore, decreased levels of TJ proteins, including occludin and claudin-5, as well as widened TJ gap with perivascular swelling are observed at the ultrastructural level in the mouse brain after ischemic preconditioning, and these effects can be prevented by tail vein injection of an ERK1/2 inhibitor (Shin et al., 2015). Taken together, these lines of evidence suggest that MKP-1 activation may be helpful in alleviating MAPK-dependent BBB breakdown. In this study, we explored the effect of EC-specific MKP-1 overexpression on ischemia-induced BBB and brain tissue injury, as well as neurological deficit, and the mechanism underlying BBB breakdown involving MAPK and TJs signaling in ischemic stroke.

Methods

Animals and study design

A total of 130 young (7- to 8-week-old, 24–26 g body weight) male C57BL/6J wide-type mice were purchased from GemPharmatech Co., Ltd. (Nanjing, Jiangsu Province, China). Among them, 24 were excluded due to death after surgery, absence of neurological deficits, or failure to complete the behavioral evaluation. All animals were handled in accordance with the guidelines provided by the Animal Center of Luohu Hospital, and the experimental protocols were approved by the Experimental Animal Ethics Committee of Luohu Hospital (No. 20210901-SZY, approval date September 1, 2021). Mice were maintained on a 12/12-hour light/dark cycle and allowed *ad libitum* access to food and water. All animals were housed at a maximum of five per cage in specific pathogen-free conditions and were allowed to acclimate to the housing conditions for at least 1 week before use. All experimental procedures were carried out during the daytime (light cycle). The animals were randomly allotted into groups. Randomization and treatment were carried out by the same person, who did not communicate the group assignments to the other examiners or data analysts. A detailed description of the *in vivo* study design and animal allocations are presented in **Additional Figure 1** and **Additional Table 1**, respectively.

In vivo model of ischemic stroke

Transient middle cerebral artery occlusion (tMCAO) surgery was performed as described previously (Bu et al., 2021). Briefly, inhalation anesthesia was administered as air containing isoflurane (4% isoflurane within 2–3 minutes for induction, 1.2–1.5% isoflurane for maintenance during surgery, RWD Life Science, Shenzhen, Guangdong Province, China, Cat# R510-22-8), and a heating pad was used to maintain body temperature at 36.5°C. The right common carotid artery, external carotid artery, and internal carotid artery were isolated. Then, an intraluminal filament (coating diameter 0.20–0.21 mm, coating length 3–4 mm, RWD Life Science, Cat# MSMC21B120PK50) was advanced from the external carotid artery stump into the internal carotid artery. One hour after occlusion, mice were re-anesthetized, and the brains were re-perfused by suture withdrawal. Mice then received softened chow and intraperitoneal injection of normal saline for 5 days.

Lentivirus administration *in vivo*

To over express MKP-1 specifically within ECs, lentiviral vectors carrying MKP-1 (Dusp1) under the control of the endothelial promotor Tie1 (pLV[Exp]-EGFP:T2A:Puro-Tie1>mDusp1) and control vectors without MKP-1 were constructed by Vectorbuilder Inc. (Guangzhou, Guangdong Province, China, Cat# VB211015-1395ekb). The lentivirus concentration was adjusted to > 1×10^9 transduction units/mL prior to delivery. Lentiviral vectors were injected into the brain 5 days before tMCAO as described previously (Bu et al., 2019, 2021). Briefly, a four-point injection was carried out at the following coordinates: (i) 0.5 mm anterior to the bregma, 2.0 mm lateral to the sagittal suture at the ipsilateral side of tMCAO, 1.0 mm from the surface of the skull; (ii) 0.5 mm anterior to the bregma, 2.0 mm lateral to the sagittal suture at the ipsilateral side of tMCAO, 2.8 mm from the surface of the skull; (iii) 0.5 mm anterior to the bregma, 3.0 mm lateral to the sagittal suture at the ipsilateral side of tMCAO, 1.0 mm from the surface of the skull; and (iv) 0.5 mm anterior to the bregma, 3.0 mm lateral to the sagittal suture at the ipsilateral side of tMCAO, 2.8 mm from the surface of the skull (Bu et al., 2019, 2021). One microliter of lentivirus was injected into each position at a rate of 0.5 μL/min with a 30-gauge needle.

In vitro model and study design

Primary human brain microvascular ECs (HBMECs, Cat# CTCC-161-HUM) were purchased from and identified by Meisen Cell Technology Co. Ltd. (Jinhua, Zhejiang Province, China), subcultured, and placed in liquid nitrogen for long-term storage. Cells were grown in EC medium (ScienCell Research Laboratories, Carlsbad, CA, USA, Cat# 1001) comprising basal medium, 5% fetal bovine serum (FBS), 1% endothelial growth supplement, and 1% penicillin/streptomycin. All cells were maintained at 37°C in a humidified incubator with 5% CO_2. To mimic ischemia, an OGD model was established as previously described (Shi et al., 2017). Briefly, cells were incubated in glucose$^-$/FBS$^-$ medium (ScienCell Research Laboratories, Cat# 1001-GF) and placed in a hypoxic chamber (Billups-Rothenberg, Del Mar, CA, USA, Cat# MIC-101) with 5% CO_2-balanced N_2 at 37°C for 1 hour. Cells were then returned to 95% air and 5% CO_2, and glucose$^+$/FBS$^+$ medium (reperfusion). Control cells were maintained in glucose$^+$/FBS$^+$ medium and air for the same. Passage 7 cells were used in all groups. To investigate downstream signaling of MKP-1 *in vitro*, HBMECs were cultured with 1 μM of the MKP-1 inhibitor (Korotchenko et al., 2014) BCI (MedChemExpress, Shanghai, China, Cat# HY-115502) or 10 nM of the ERK1/2 inhibitor (Blake et al., 2016) ravoxertinib (MedChemExpress, Cat# HY-15947) during and after OGD. The chemicals were dissolved in 0.1% dimethyl sulfoxide. An equal amount of dimethyl sulfoxide was used as vehicle control. A detailed description of *in vitro* study design is presented in **Additional Figure 1**.

Immunofluorescence staining

Three days after tMCAO, mice were deeply anesthetized with 5% isoflurane and transcardially perfused with phosphate-buffered saline followed by 4% (v/v) paraformaldehyde (PFA). The whole brain was post-fixed in 4% PFA overnight and then transferred to a 30% (w/v) sucrose solution for 48 hours. The brain was sliced into 30-μm-thick coronal sections that were incubated in 0.1% Triton X-100 for 15 minutes, followed by 1 hour of antigen blocking in 1% bovine serum albumin (Solarbio Science & Technology, Beijing, China, Cat# SW3015) at 25°C. To detect MKP-1 expression, sections were incubated with rabbit anti-MKP-1 antibody (1:500, Thermo Fisher Scientific, Waltham, MA, USA, Cat# PA5-105274, RRID: AB_2853876) overnight at 4°C followed by anti-rabbit secondary antibody (Alexa Fluor 488, 1:1000, Abcam, Cambridge, UK, Cat# ab150073, RRID: AB_2636877) for 1 hour at 25°C. In addition, 200 μL of tomato lectin (0.5 mg/mL, DyLight 594, Thermo Fisher Scientific, Cat# L32471), a blood vessel marker (Robertson et al., 2015), was injected through the tail vein 30 minutes prior to animal sacrifice. Impairment of BBB integrity was assessed by immunohistochemistry for mouse immunoglobulin (Ig) G (Ehrlich et al., 2012; Zong et al., 2020), as circulating IgG accumulates in the brain parenchyma and is detectable in the case of BBB disruption (Min et al., 2019). Sections were incubated with anti-mouse IgG antibody (Alexa Fluor 594, 1:1000, Thermo Fisher Scientific, Cat# A32742, RRID: AB_2762825) for 1 hour at 25°C. The nuclei were stained using 4′,6-diamidino-2-phenylindole (Abcam, Cat# ab104139).

Twelve hours after OGD, HBMECs grown on collagen-coated coverslips in 12-well culture plates were fixed with 4% PFA for 15 minutes followed by blocking with 1% bovine serum albumin for 1 hour at 25°C. The cells were then incubated with the following primary antibodies overnight at 4°C: rabbit anti-cleaved caspase-3 (Asp175) (1:400, Cell Signaling Technology, Danvers, MA, USA, Cat# 9661S, RRID: AB_2341188) and rabbit anti-occludin (1:400, Cell Signaling Technology, Cat# 91131S). After rinses in phosphate-buffered saline, the cells were incubated with anti-rabbit secondary antibodies conjugated with Alexa Fluor 594 (1:1000, Thermo Fisher Scientific, Cat# A11012, RRID: AB_2534079) or Alexa Fluor 488 (1:1000, Abcam, Cat# ab150073, RRID: AB_2636877) for 1 hour at 25°C. Finally, the coverslips were treated with anti-fade solution containing 4′,6-diamidino-2-phenylindole and mounted on glass slides.

Fluorescence images were captured with a confocal microscope at 40× magnification. Regions of interest were randomly selected from the similar coordinates of brain coronal slices among the groups. We considered the tissue area within 1.5 mm of the infarct core to be the peri-infarct area (Agulla et al., 2013; Bu et al., 2021). Integrated optical density was calculated using ImageJ software (V1.52e, National Institutes of Health, Bethesda, MD, USA), and the results were normalized by dividing each value by the mean integrated optical density of the control group.

Infarct volume measurement

On day 3 after tMCAO, the mouse brains were removed, frozen at −80°C for 5 minutes and then sliced into five coronal sections (2-mm thickness). The sections were stained for 15 minutes at 37°C with 1.5% 2,3,5-triphenyltetrazolium chloride monohydrate (Sigma-Aldrich, St. Louis, MO, USA, Cat# T8877) and fixed with 4% PFA. The infarct volume was then calculated as previously described (Liu et al., 2014). Briefly, section images were captured with a bright field microscope (Leica, Wetzlar, Germany, Cat# M80), and the infarct volumes were measured using ImageJ software.

Western blot analysis

Microvessels were extracted from the injured hemisphere 3 days after tMCAO according to an established approach (Yin et al., 2010). Microvessel protein was collected in 1× NP-40 buffer (Solarbio Science & Technology, Cat# N8032) containing 1 mM phenylmethanesulfonyl fluoride, protease

inhibitor (MedChemExpress, Cat# HY-K0010) and phosphatase inhibitor (MedChemExpress, Cat# HY-K0021), and sonicated for 10 seconds. Tissue lysate was centrifuged at 20,000 × *g* for 20 minutes at 4°C, and the protein-containing supernatant was collected. Protein concentration was measured by bicinchoninic acid assay (Beyotime Biotechnology, Shanghai, China, Cat# P0012). Equal amounts of protein (30 μg) were loaded onto 10% precast protein gels (Beyotime Biotechnology, Cat# P0456M) for electrophoresis. After that, proteins were transblotted to polyvinylidene fluoride membranes and blocked with 5% skim milk for 1 hour at 25°C. Next, the membranes were exposed to primary antibodies against T202/Y204 phosphorylated ERK1/2 (1:2000, Cell Signaling Technology, Cat# 4370S, RRID: AB_2315112), ERK1/2 (1:2000, Cell Signaling Technology, Cat# 4695S, RRID: AB_390779), Thr180/Tyr182 phosphorylated P38 (1:1000, Cell Signaling Technology, Cat# 4631S, RRID: AB_331765), P38 (1:1000, Cell Signaling Technology, Cat #8690S, RRID: AB_10999090), occludin (1:1000, Cell Signaling Technology, Cat# 91131S), and β-actin (1:1000, Cell Signaling Technology, Cat# 4970S, RRID: AB_2223172) for 1 hour at 25°C. Once excess primary antibody was washed off with Tris-buffered saline containing Tween 20, the membranes were incubated with anti-rabbit horseradish peroxidase-linked secondary antibody (1:4000, Cell Signaling Technology, Cat# 7074S, RRID: AB_2099233) for 1 hour at 25°C. Relative protein expression was normalized to β-actin. Optical density was captured with a Bio-Rad imaging system (Hercules, CA, USA, Cat# ChemlDoc).

Survival rate

Before and after tMCAO, the percentage of surviving animals in each group was recorded each day to determine the survival rate.

Behavioral tests

To assay functional recovery after stroke, we performed a battery of behavioral tests including: (1) neurological deficit score (NDS) as a measure of overall neurological deficits, (2) novel objective recognition test (NORT) for memory/cognitive function, (3) adhesive removal test (ART) for sensorimotor function, and (4) wire hanging test (WHT) for grip strength. We performed NDS at 3 days, ART and WHT at 3, 7, and 14 days, and NORT at 14 days after tMCAO. Baseline performance in each test was assayed prior to tMCAO.

NDS

The Bederson score system, with minor modifications, was employed to assess neurological deficit (Bieber et al., 2019): 0 = no deficit, 1 = forelimb flexion, 2 = circling to the left, 3 = decreased resistance to lateral push, and 4 = no spontaneous walking with reduced level of consciousness (the most severe).

NORT

This test is based on the tendency of mice to interact more with a novel object than with a familiar object, which enables investigation of memory deficits after stroke (Bevins and Besheer, 2006). Briefly, animals were allowed to explore an arena containing two identical objects for 5 minutes (trial 1). After a 5-minute interval in a feeding cage, mice were placed in the same arena where one of the objects had been replaced with a novel object, for another 5-minute exploration (trial 2). The time spent at both objects was recorded in seconds, and the discrimination index was calculated as follows: (TNtrial2/TFtrial2)/(TFtrial1/TFtrial1), in which TN indicates the time spent at the novel object and TF indicates the time spent at the familiar object.

ART

To measure sensorimotor deficits, adhesive-backed tape (25 mm^2) was used as tactile stimulus, placed on the distal-radial region of the left wrist. Elapsed time from tape adhesion to tape removal in three trials was averaged (Bu et al., 2021).

WHT

To measure post-stroke limb strength and balance, WHT was performed using a wire cage top (18 cm × 9 cm in size) that was held 90 cm above a cage containing soft bedding. Mice were monitored for up to 120 seconds, and the latency to fall from the inverted cage top was recorded in seconds (Ruan and Yao, 2020).

Enzyme-linked immunosorbent assay

Three days after tMCAO, the ipsilateral hemisphere was collected from each mouse. Tissue homogenate was prepared as described previously (Al Mamun et al., 2018). The levels of cytokines, including interleukin (IL)-1β (Thermo Fisher Scientific, Cat# BMS6002), IL-6 (Thermo Fisher Scientific, Cat# BMS603-2), tumor necrosis factor (TNF)-α (Thermo Fisher Scientific, Cat# BMS607-3) using, and chemokine C-C motif ligand (CCL)-2 (Thermo Fisher Scientific, Cat# BMS6005), were measured by commercially available enzyme-linked immunosorbent assay kits according to manufacturers' instructions.

Assessment of cell viability and BBB impairment

Cell viability was assessed by cell counting kit-8 (CCK-8, APExBIO, Houston, TX, USA, Cat# K1018-1) according to the manufacturer's protocol. Briefly, CCK-8 reagent was added to the cell culture medium at a ratio of 1:10, followed by incubation for 1 hour. The absorbance of each well at 450 nm was determined an automatic microplate reader (BioTek, Winooski, VT, USA, Cat# Synergy H1M).

EC monolayers are a well-accepted *in vitro* BBB model that is used to precisely assess barrier permeability (Paradis et al., 2016). In this study, an HBMEC monolayer was established in transwell inserts as described previously, with minor modifications (Shi et al., 2016). Briefly, the transwell polyethylene terephthalate membranes (0.4-μm pore, Corning Incorporated, Corning, NY, USA, Cat# 3460) were coated with collagen (10 μg/mL, Corning Incorporated, Cat# 354265) and fibronectin (20 μg/mL, Corning Incorporated, Cat# 356008). HBMECs were seeded onto the membrane and grown until they reached confluence. To assess paracellular permeability, fluorescein isothiocyanate-dextran (70 kDa, Sigma-Aldrich, Cat# 46945) was added to the luminal chamber at a concentration of 1 μM in 300 μL EC medium. The fluorescence intensity of 30 μL of medium collected from the larger chamber was measured with a fluorescence reader (BioTek, Cat# H1M) before and 1, 3, and 6 hours after OGD. The medium in the larger chamber was replaced (700 μL) 30 minutes before each time point. The results were normalized by dividing each value by the mean of the pre-OGD values from the phosphate-buffered saline control group.

Statistical analysis

The results are presented as mean ± standard error of mean (SEM). Data were analyzed by GraphPad Prism (version 9.0.0 for Windows, GraphPad Software, San Diego, CA, USA, www.graphpad.com). Normal distribution and homogeneity of variance were examined by the Kolmogorov-Smirnov test. Unpaired *t*-test was used for comparisons between two individual groups. One-way analysis of variance followed by Bonferonni multiple comparisons test was applied for comparisons across multiple groups. Significant differences were defined as $P < 0.05$. Sample size was not calculated in this study. Instead, the number of animals used in this study was calculated based on the power analysis used for similar experiments in our earlier study (Liu et al., 2018).

Results

MKP-1 overexpression in ECs ameliorates ischemic brain injury

To elucidate the specific role of MKP-1 expression in ECs, lentiviral vector encoding MKP-1 under the control of the endothelial promotor Tie1 was injected into the ischemic side of the brain. Five days after injection, isolated microvessel homogenate was prepared to validate MKP-1 overexpression by western blot assay. We found that MKP-1 expression was significantly enhanced in the Tie1-MKP-1 group compared with the control vector group ($P < 0.01$; **Figure 1A**). MKP-1 overexpression was confirmed by immunofluorescence staining, as an increase in MKP-1 expression in microvessels (lectin$^+$) was observed in the Tie1-MKP-1 group compared with the control group ($P < 0.05$; **Figure 1B**). To evaluate the effect of MKP-1 on brain injury, infarct size was measured 3 days after tMCAO. As expected, MKP-1 overexpression significantly reduced infarct size compared with the control vector group ($P < 0.05$; **Figure 1C**).

MKP-1 overexpression in ECs promotes sensorimotor and memory/cognitive function recovery after ischemia

We next investigated whether EC-specific MKP-1 overexpression can improve post-stroke outcomes. The survival rate was not markedly altered up to 14 days after stroke (**Figure 2A**). However, stroke-induced neurological deficit was attenuated by EC-specific MKP-1 overexpression compared with the control group ($P < 0.05$; **Figure 2B**). Three types of behavioral tests were performed to comprehensively evaluate sensorimotor and memory/cognitive functions (**Figure 2C–E**). In the control group, sensorimotor deficiencies (as assessed by ART and WHT) were the most prominent at 3 days after tMCAO, followed by gradual recovery. The mice in the MKP-1 overexpression group exhibited significantly better performance than the control group starting from 3 days after tMCAO in the ART test ($P < 0.01$; **Figure 2C**), and starting 7 days after tMCAO in the WHT test ($P < 0.05$; **Figure 2D**), although their scores recovered to levels comparable to those of the control mice within 14 days. Furthermore, ECs-specific MKP-1 overexpression improved memory/cognitive function recovery, as assayed by NORT, at 14 days after tMCAO ($P < 0.05$; **Figure 2E**).

MKP-1 overexpression in ECs mitigates ischemia-induced microvessel destruction and BBB impairment

Cerebral microvessel destruction and BBB impairment after stroke are the key factors causing secondary brain injury (Arai et al., 2011). Therefore, to investigate the role of EC-specific MKP-1 expression in vascular integrity, we visualized microvessels by intravenous injection of lectin conjugated with DyLight 594 and quantified MKP-1 and lectin coexpression 3 days after tMCAO. We found that ischemia induced blood vessel destruction in the peri-infarct zone, as evidenced by a reduction in lectin signal intensity compared with the sham group ($P < 0.01$; **Figure 3A**). EC-specific MKP-1 overexpression protected against vessel destruction compared with the control vector group ($P < 0.05$). Next, the effect of EC-specific MKP-1 on BBB leakage was investigated. Ischemia increased BBB permeability, which was reflected by the increase in IgG signal intensity compared with the sham group ($P < 0.001$; **Figure 3B**). As expected, EC-specific MKP-1 overexpression ameliorated stroke-induced BBB leakage compared with the control vector group ($P < 0.01$).

Circulating neutrophils and macrophages can infiltrate through the disrupted BBB within hours of an ischemic event and produce pro-inflammatory cytokines, such as IL-1, IL-6, and TNF-α. This induces the release of chemokines such as CCL-2 from brain tissue (An et al., 2014; Jayaraj et al., 2019), leading to expansion of the infarct area. We hypothesized that the protective effect of EC-specific MKP-1 overexpression on BBB integrity would

alleviate this inflammatory reaction. We measured a panel of inflammatory cytokines and chemokines in ischemic brain parenchyma 3 days after tMCAO. Indeed, tMCAO led to a significant increase in the expression of markers of inflammation, including IL-1β, IL-6, TNF-α, and CCL-2 (all $P < 0.001$; **Figure 3C**). EC-specific MKP-1 overexpression alleviated the increase in IL-1β, IL-6, and CCL-2 expression compared with the control vector group (all $P < 0.05$). However, TNF-α expression levels were not altered by MKP-1 overexpression.

EC-specific MKP-1 overexpression alleviates MAPK signaling activation and TJ protein downregulation in the ischemic brain

Next, we investigated the molecular mechanism of the microvascular protection exerted by EC-specific MKP-1 overexpression. ERK1/2 and P38 have been considered as the detrimental effectors in mediating brain injury at the early stage of ischemic stroke (Sun and Nan, 2016). Thus, we assessed ERK1/2 and P38 expression in ECs overexpressing MKP-1 at 3 days after tMCAO. We found that ischemia significantly induced phosphorylation of ERK1/2 (Thr202/Tyr204) ($P < 0.05$), but not P38 (Thr180/Tyr182), compared with the sham group (**Figure 4**). EC-specific MKP-1 overexpression prevented the upregulation of phosphorylated ERK1/2 ($P < 0.05$). Total ERK1/2 and P38 expression levels were not altered. In addition, occludin expression decreased after tMCAO ($P < 0.01$; **Figure 4**), and this effect was reversed by EC-specific MKP-1 overexpression ($P < 0.05$). These results suggest that alleviation of stroke-induced downregulation of occludin expression may be associated with ERK1/2 deactivation by MKP-1.

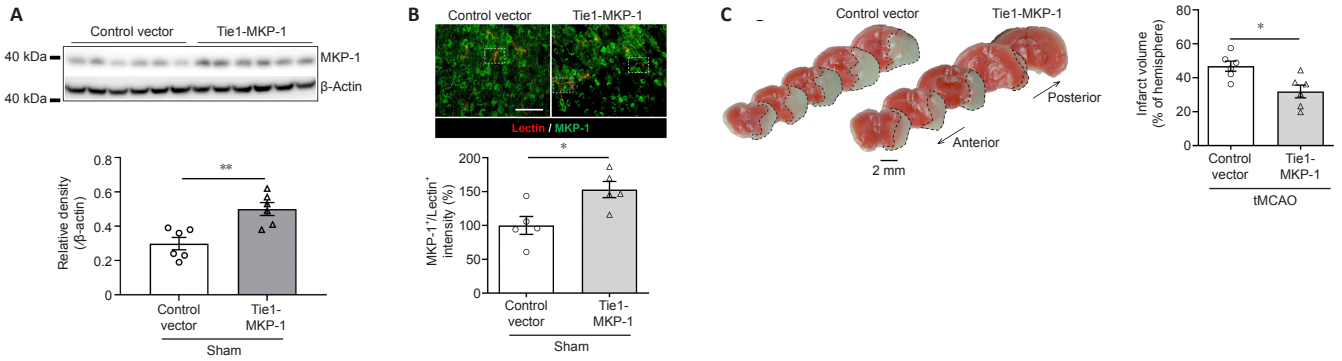

Figure 1 | **Effect of ECs-MKP-1 overexpression on ischemic brain injury.**

Lentiviral vectors encoding MKP-1 and the endothelial cell-specific promotor Tie1 were injected into the cerebral cortex and striatum on the stroke side to overexpress MKP-1 within ECs in mice. The same process was performed using lentivirus without the MKP-1 sequence as a control. (A, B) Western blotting (A; $n = 6$/group) and immunohistochemistry (B; $n = 5$/group) were performed 5 days after lentiviral injection to validate MKP-1 overexpression in ECs. The area surrounded by a dotted line indicates lectin$^+$/MKP-1$^+$ staining. (C) Cerebral infarction volume was assayed by 2,3,5-triphenyltetrazolium chloride staining 3 days after tMCAO ($n = 6$/group). Scale bars: 100 μm (B), 2 mm (C). All values are shown as mean ± SEM. *$P < 0.05$, **$P < 0.01$ (unpaired t-test). EC: Endothelial cell; MKP-1: mitogen-activated protein kinase phosphatase-1; tMCAO: transient middle cerebral artery occlusion.

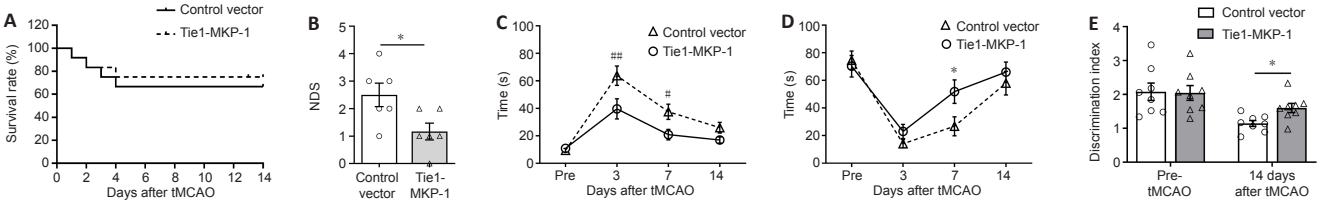

Figure 2 | **Effect of endothelial cells-MKP-1 overexpression to post-stroke outcomes.**

(A) Survival rate ($n = 12$/group). (B) Neurological deficit was assayed by neurological deficit score ($n = 6$/group, unpaired t-test). (C, D) Sensorimotor function was assayed by (C) adhesive removal test and (D) wire hanging test ($n = 8$/group, one-way analysis of variance followed by Bonferonni multiple comparisons test). (E) Memory/cognitive function was assessed by novel object recognition test ($n = 8$/group, one-way analysis of variance followed by Bonferonni multiple comparisons test). All values are shown as mean ± SEM. *$P < 0.05$; #$P < 0.05$, ##$P < 0.05$, *vs*. Tie1-MKP-1 group. MKP-1: Mitogen-activated protein kinase phosphatase-1; tMCAO: transient middle cerebral artery occlusion.

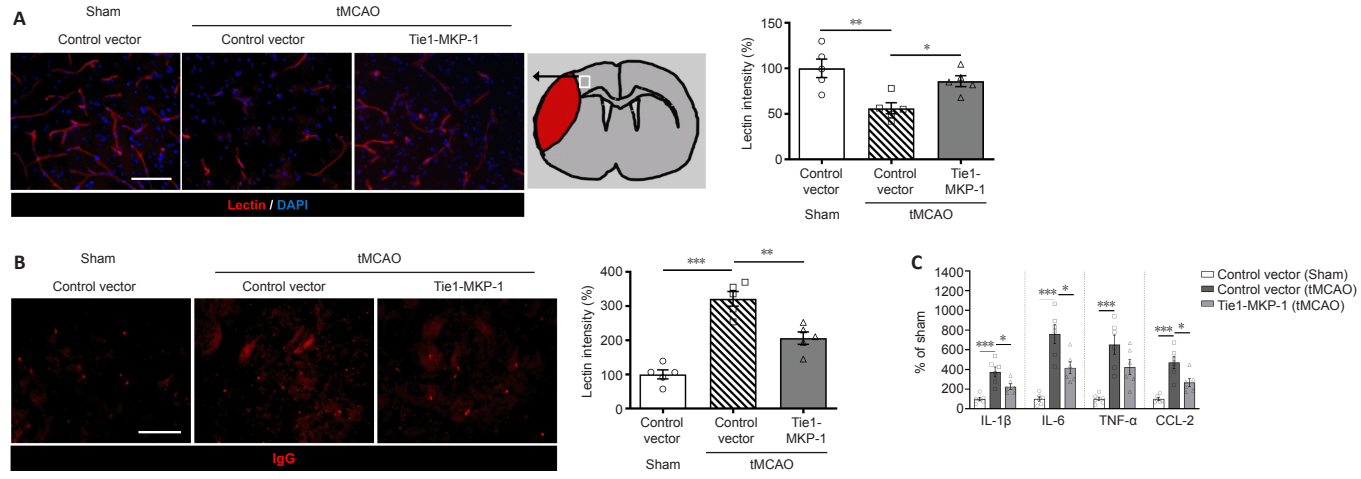

Figure 3 | **Effect of EC-MKP-1 overexpression on stroke-induced cerebrovascular destruction.**

(A-left) Representative images showing immunofluorescence of the EC marker lectin (red, DyLight 594) and the nuclear marker DAPI (350 nm). Schematic diagram of a coronal section of mouse brain; the infarct core is shown in red area. Fluorescence images were captured of the peri-infarct zone, which is indicated by the white box. (A-right) Statistical analysis of lectin signal intensity ($n = 5$/group). (B-left) Representative images showing IgG immunofluorescence (red, Alexa Fluor 594). (B-right) Statistical analysis of IgG signal intensity ($n = 5$/group). Scale bars: 100 μm. (C) Levels of pro-inflammatory markers were measured in the ischemic hemisphere 3 days after tMCAO by enzyme-linked immunosorbent assay ($n = 6$/group). All values are shown as mean ± SEM. *$P < 0.05$, **$P < 0.01$, ***$P < 0.001$ (one-way analysis of variance followed by Bonferonni multiple comparisons test). CCL-2: Chemokine C-C motif ligand-2; DAPI: 4′,6-diamidino-2-phenylindole; EC: endothelial cell; IL: interleukin; MKP-1: mitogen-activated protein kinase phosphatase-1; tMCAO: transient middle cerebral artery occlusion; TNF-α: tumor necrosis factor-α.

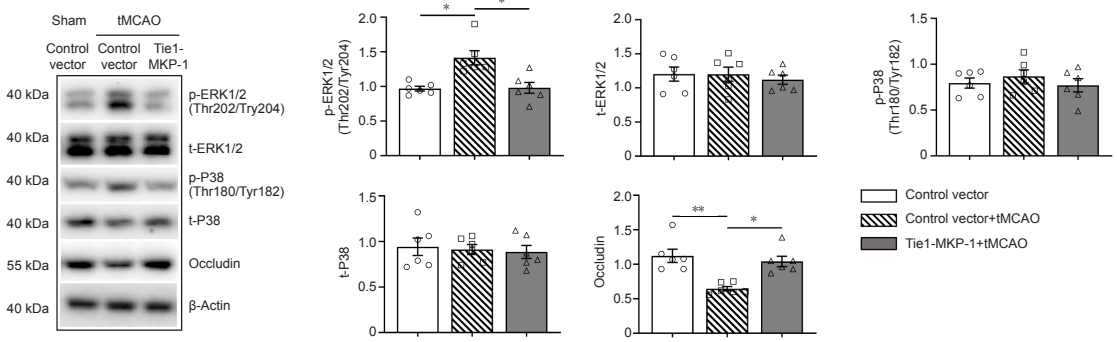

Figure 4 | **Effect of EC-MKP-1 overexpression on microvessel MAPK and occludin expression levels.**
Western blotting was performed to quantify the relative intensity of proteins of interest, including p-ERK1/2 (Thr202/Tyr204), t-ERK1/2, p-P38 (Thr180/Tyr182), t-P38, and occludin, normalized to β-actin. All values are shown as mean ± SEM (n = 6/group). *P < 0.05, **P < 0.01 (one-way analysis of variance followed by Bonferonni multiple comparisons test). EC: Endothelial cell; MKP-1: mitogen-activated protein kinase phosphatase-1; p-ERK1/2: phosphorylated extracellular-regulated protein kinases 1/2; p-P38: phosphorylated P38; t-ERK1/2: total extracellular-regulated protein kinases 1/2; t-P38: total P38; tMCAO: transient middle cerebral artery occlusion.

Inhibiting MKP-1 worsens OGD-induced BBB leakage by reactivating ERK1/2 *in vitro*

Given that Tie1 has been detected in human and rat platelets (Fujikawa et al., 1999), it is possible that the Tie1-MKP-1 vector-mediated BBB protection that we observed *in vivo* may be due to MKP-1 expression within platelets. To rule out this possibility, we confirmed the role of EC-specific MKP-1 expression in an *in vitro* BBB model. An EC monolayer was subjected to 60-minute OGD, and the transit of fluorescent tracers (fluorescein isothiocyanate-dextran, 70 kDa) through the monolayer was evaluated. Compared with normoxic conditions, OGD induced significant leakage through the monolayer, as evidenced by an increase in the concentration of the fluorescent tracer in the abluminal medium 6 hours after OGD (P < 0.001; **Figure 5A**). Importantly, perfusion with 1 μM of the MKP-1 inhibitor BCI progressively worsened barrier leakage compared with vehicle control group (P < 0.01 at 3 hours, P < 0.001 at 6 hours), which is in line with our *in vivo* results. We then explored pathways downstream of MKP-1. ERK1/2 inhibition with 10 nM ravoxertinib significantly alleviated monolayer leakage (P < 0.01 at 6 hours). In addition, occludin expression was measured 12 hours after OGD by immunofluorescence assay. The OGD-induced reduction in occludin expression was worsened by BCI (P < 0.01; **Figure 5B**) and alleviated by ravoxertinib (P < 0.05) compared with the vehicle groups. Interestingly, co-incubating cells with MKP-1 and ERK1/2 inhibitors had the same effect on barrier permeability and occludin expression as treatment with ERK1/2 inhibitor alone, suggesting that MKP-1 protects against BBB leakage by deactivating ERK1/2.

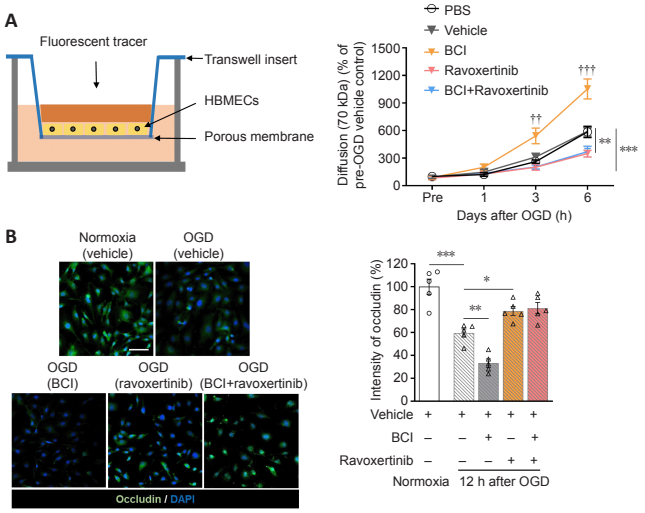

Figure 5 | **Effect of inhibiting MKP-1-ERK1/2 signaling on BBB permeability *in vitro*.**
HBMECs were subjected to 60 minutes of OGD followed by reperfusion for 6 hours. The cells were incubated with 1 μM of the MKP-1 inhibitor BCI and 10 nM of the ERK1/2 inhibitor ravoxertinib during and after OGD; 0.1% DMSO was used as the drug vehicle. The same volume of PBS was used for the blank control group. (A) Permeability of the HBMEC monolayer in the transwell insert. The concentration of the fluorescent tracer (fluorescein isothiocyanate-dextran, 70 kDa) in the larger chamber was quantified pre-OGD and 1, 3, and 6 hours after OGD (n = 6/group). (B) The intensity of occludin expression (green, Alexa Fluor 488) in HBMECs was quantified 12 hours after OGD. The signal in the drug vehicle group was quantified pre-OGD and used as the baseline value. DAPI (blue) was used as a nuclear marker (n = 5/group). Scale bar: 50 μm. All values are shown as mean ± SEM. *P < 0.05, **P < 0.01, ***P < 0.001. ††P < 0.01, †††P < 0.001, *vs.* vehicle group (one-way analysis of variance followed by Bonferonni multiple comparisons test). BBB: Blood-brain barrier; DAPI: 4′,6-diamidino-2-phenylindole; DMSO: dimethyl sulfoxide; ERK1/2: extracellular-regulated protein kinases 1/2; HBMEC: human brain microvascular endothelial cell; MKP-1: mitogen-activated protein kinase phosphatase-1; OGD: oxygen and glucose deprivation; PBS: phosphate-buffered saline.

Inhibiting MKP-1 worsens OGD-induced cell death by reactivating ERK1/2 *in vitro*

We next asked whether MKP-1-ERK1/2 signaling regulates EC viability. Neither 1 μM BCI nor 10 nM ravoxertinib altered cell viability under normoxic conditions, as determined by CCK-8 assay (**Figure 6A**), suggesting that MKP-1 and ERK1/2 inhibition were not cytotoxic. Similar to a previous study (Bu et al., 2019), OGD induced significant cell death (P < 0.001; **Figure 6A**) as well as caspase-3 cleavage, an essential sign of programmed cell death (Porter and Jänicke, 1999) (P < 0.001; **Figure 6B**) at 12 hours after OGD. Importantly, incubation of ECs with BCI further reduced cell viability compared with the vehicle group (CCK-8: P < 0.001; cleaved caspase-3: P < 0.01), whereas ravoxertinib significantly salvaged cells (CCK-8: P < 0.05; cleaved caspase-3: P < 0.05). There was no significant difference between cells treated with both BCI and ravoxertinib and cell treated with ravoxertinib alone.

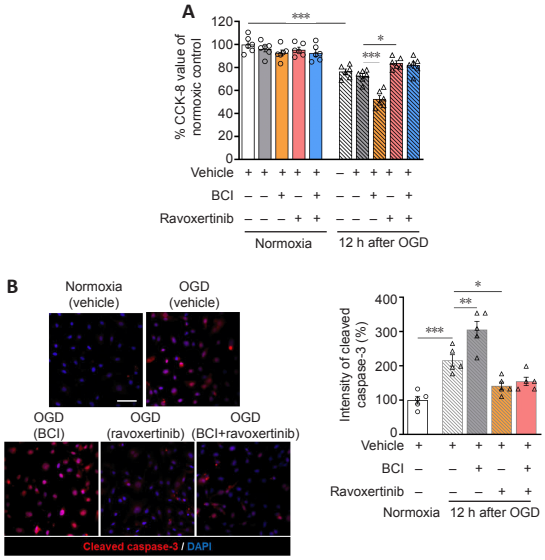

Figure 6 | **Effect of inhibiting MKP-1-ERK1/2 signaling on HBMEC viability *in vitro*.**
HBMECs were subjected to 60 minutes of OGD followed by reperfusion. The cells were treated with 1 μM of the MKP-1 inhibitor BCI and 10 nM of the ERK1/2 inhibitor ravoxertinib during and after OGD; 0.1% DMSO was used as the drug vehicle. Cells were maintained in glucose$^+$/FBS$^+$ medium with 95% air as the normoxic control. (A) Assessment of endothelial cell viability by CCK-8 (n = 6/group). (B) Cleaved caspase-3 (Asp175) expression (red, Alexa Fluor 594) was assessed by immunofluorescence. DAPI (blue) was used as a nuclear marker (n = 5/group). Scale bar: 50 μm. All values are shown as mean ± SEM. *P < 0.05, **P < 0.01, ***P < 0.001 (one-way analysis of variance followed by Bonferonni multiple comparisons test). CCK-8: Cell counting kit-8; DAPI: 4′,6-diamidino-2-phenylindole; DMSO: dimethyl sulfoxide; ERK1/2: extracellular-regulated protein kinases 1/2; FBS: fetal bovine serum; HBMEC: human brain microvascular endothelial cell; MKP-1: mitogen-activated protein kinase phosphatase-1; OGD: oxygen and glucose deprivation.

Discussion

In this study, we revealed an EC-specific role for MKP-1 in protecting against ischemia-induced brain injury. EC-specific MKP-1 overexpression prevented microvessel ERK1/2 activation and occludin downregulation, as well as BBB breakdown induced by ischemic stroke in mice. By preserving BBB integrity, EC-specific MKP-1 overexpression reduced cerebral pro-inflammatory factor production and expansion of brain infarct area, and these effects were

accompanied by improved post-stroke recovery. Furthermore, mechanistic investigation showed that inhibition of MKP-1 worsened the EC barrier leakage, cell death, and occludin downregulation induced by OGD, whereas inhibition of ERK1/2 had the opposite effect. Finally, co-inhibition of MKP-1 and ERK1/2 had no additive effect compared with inhibition of ERK1/2 alone, suggesting that MKP-1 preserves BBB integrity via deactivating ERK1/2.

How does EC-specific MKP-1 improve functional recovery after ischemia? BBB breakdown is usually associated with high mortality and worsens clinical consequences after stroke (Rodrigues and Granger, 2015). A preclinical study demonstrated that blocking early BBB dysfunction by manipulating endothelial genes can provide parenchymal protection and improve long-term functional outcomes (Jiang et al., 2018). In the present study, we found that EC-specific MKP-1 overexpression by lentivirus reversed stroke-induced microvessel damage. This effect was accompanied by improved behavioral recovery, suggesting that EC-specific MKP-1 improves post-stroke outcomes by protecting the integrity of the BBB. It is worth noting that, in addition to protecting against microvessel damage, MKP-1 can also improve neovascularization. In a murine model of hind limb ischemia, genomic deletion of Dusp1 blunted angiogenesis and microvascular arteriogenesis (Boerckel et al., 2014). In addition, cell-type specific deletion of Dusp1 abrogated vascular endothelial growth factor-induced migration and tube formation and reduced proliferation in cultured ECs (Kinney et al., 2008). In the present study, Tie1-MKP-1 lentivirus was injected into the brain parenchyma, where continually augmented MKP-1 production during both the acute phase (tissue injury) and chronic phase (tissue remodeling) after stroke, and may have promoted neovascularization to some extent. However, the exact role of MKP-1 in neovascularization after cerebral ischemia requires further investigation.

To understand the role of MKP-1 downstream signaling in ECs in mediating BBB integrity, we isolated brain microvessels and determined the expression levels of MKP-1 substrates, including ERK1/2 and P38, in response to stroke insult in mice. We found that stroke induces phosphorylation of ERK1/2 (T202/Y204) but not P38 (Thr180/Tyr182), and that this effect was robustly prevented by MKP-1 overexpression. We then investigated the causal relationship between MKP-1 and ERK1/2 within ECs *in vitro*. We found that the downregulation of occludin and the increase in EC barrier permeability after OGD were worsened by pharmacological inhibition of MKP-1. ERK1/2 inhibition had a beneficial effect, unlike MKP-1 inhibition, and co-inhibition of MKP-1 and ERK1/2 had no addictive effect compared with inhibition of ERK1/2 alone, suggesting that MKP-1 preserves BBB integrity via deactivating ERK1/2 during ischemia. Interestingly, although ERK1/2 and P38 have high homology (Sun and Nan, 2016), MKP-1 deletion augments p38, but not ERK1/2, activation in cerebral microglia during the acute phase of ischemic stroke in mice (Liu et al., 2014). This difference is probably due to the cell-type specific preference of MKP-1 for diverse members of the MAPK family.

How MKP-1–ERK1/2 signaling influences occludin expression is not well addressed here, but Sma and Mad protein (SMAD) 3/4 is likely to be involved. SMAD3/4 can co-repress the occludin promoter in epithelial cells (Vincent et al., 2009), and ERK1/2 activation can induce SMAD3 phosphorylation (Qing et al., 2014). In this case, we assume that the inhibitory activity of MKP-1 toward ERK1/2 may prevent SMADs from binding to the occludin promotor, resulting in increased expression of occludin in cerebral ischemia. It is worth noting that MAPKs are able to modulate the expression of other TJ members other than occludin in multiple pathological conditions, e.g., excess salt intake and ischemic preconditioning (Shin et al., 2015; Zhang et al., 2015). More research is needed to investigate the response of TJs to MKP-1 signaling within ECs after stroke.

Ischemia-induced ECs death is a major factor involved in BBB disruption (Zille et al., 2019). Oxidative stress elicits epithelial caspase-3 cleavage, nuclear condensation, and cell apoptosis, which can be reversed by ERK1/2 inhibition (Zhuang et al., 2007). In this study, pharmacological inhibition of MKP-1 in cultured ECs aggravated OGD-induced cell death and caspase-3 cleavage (Asp175), whereas inhibition of ERK1/2 performs had the opposite effect (which was comparable to the effect of co-inhibition of MKP-1 and ERK1/2), suggesting that MKP-1 may alleviate ischemia-induced ECs death via negatively modulating ERK1/2 activity. It is worth noting that, in response to extracellular signals, ERKs coordinate a broad range of intracellular activities, ranging from motility, inflammation, and differentiation to cell death and survival (Roux and Blenis, 2004); however, the role of ERKs in stroke is still debated (Sawe et al., 2008). In contrast to the detrimental effect of ERK1/2 on ECs survival during the acute phase after ischemic stroke, as we observed here, a previous study showed that delayed perfusion with Rac1 and Pak1 inhibitors prevented ECs proliferation and migration, which was accompanied by a reduction in p-ERK1/2 and BDNF release (Bu et al., 2019), implying a positive correlation between ERK1/2 activity and microvessel reconstitution. Although the contribution of ECs ERK1/2 expression to microvessel reconstitution needs to be confirmed using pharmacological or genetic tools, it appears that microvessel modulation by MKP-1/ERK1/2 signaling relies on progress after stroke (acute *vs*. chronic phases) to some extent, and that the potential side effects of targeting MKP-1 need to be considered carefully in further translational studies.

There were several limitations to this study. First, we only studied EC-specific MKP-1 overexpression in young male mice. BBB hyperpermeability after stroke occurs much earlier and is more severe in aged subjects than in young subjects (Jiang et al., 2018), resulting in a poorer prognosis. In addition, sex differences in stroke risk are well documented. Pre-menopausal women own a survival advantage after stroke than men is predominantly attributed to the protective effects of estrogen (Manwani et al., 2013). Thus, future studies of MKP-1-mediated protection of BBB integrity and against brain injury should be conducted in both sexes and in aged subjects as well as young subjects. Even so, the efficacy of increasing EC-specific MKP-1 expression to promote post-stroke recovery in aged females may not differ from that seen in young male animals. Another limitation of the study is that post-stroke survival was not markedly altered by MKP-1 overexpression in cerebral ECs. In this study, 9 out of 12 mice in the Tie1-MKP-1 group and 8 out of 12 mice in the control vector group survived. This negligible improvement in survival conferred by Tie1-MKP-1 suggests that a larger sample size may be required, and that the modulation of post-stroke mortality by EC-specific MKP-1 overexpression may also be dependent on the severity of brain injury and on the stroke model. Last but not least, we manipulated MKP-1 expression prior to stroke insult *in vivo*, which was conducive to studying the acute phase of stroke. However, this approach is impractical for stroke treatment in a clinical setting. The effect of delayed EC-specific MKP-1 overexpression on post-stroke recovery should be addressed in the future.

In summary, this study used multiple approaches as well as *in vivo* and *in vitro* stroke models to reveal that EC-specific MKP-1 overexpression protects against BBB breakdown induced by ischemic stroke, and that this process is mediated by ERK1/2 signaling. Overexpression MKP-1 in ECs may offer a potential therapeutic strategy for protecting the brain against ischemic injury and promoting functional recovery.

Author contributions: *XDQ performed the majority of the experiments and analyzed data; TQY and JHZ performed experiments; HBC and JJJ provided technical support and data interpretation; SHQ and YC helped with manuscript proof-reading; LSX conducted experimental design and drafted manuscript; FB conceived the research project, experimental design and finalized the paper. All authors read and approved the final manuscript.*
Conflicts of interest: *The authors declare no conflicts of interest.*
Availability of data and materials: *All data generated or analyzed during this study are included in this published article and its supplementary information files.*

Open peer reviewer: *Julien Rossignol, Central Michigan University, USA.*
Additional files:
Additional Figure 1: *Schematic representation of the study design used for both in vivo (A) and in vitro (B) experimental sets.*
Additional Table 1: *Animal use.*
Additional file 1: *Open peer review report 1.*

References

Agulla J, Brea D, Campos F, Sobrino T, Argibay B, Al-Soufi W, Blanco M, Castillo J, Ramos-Cabrer P (2013) In vivo theranostics at the peri-infarct region in cerebral ischemia. Theranostics 4:90-105.

Al Mamun A, Chauhan A, Yu H, Xu Y, Sharmeen R, Liu F (2018) Interferon regulatory factor 4/5 signaling impacts on microglial activation after ischemic stroke in mice. Eur J Neurosci 47:140-149.

An C, Shi Y, Li P, Hu X, Gan Y, Stetler RA, Leak RK, Gao Y, Sun BL, Zheng P, Chen J (2014) Molecular dialogs between the ischemic brain and the peripheral immune system: dualistic roles in injury and repair. Prog Neurobiol 115:6-24.

Arai K, Lok J, Guo S, Hayakawa K, Xing C, Lo EH (2011) Cellular mechanisms of neurovascular damage and repair after stroke. J Child Neurol 26:1193-1198.

Bevins RA, Besheer J (2006) Object recognition in rats and mice: a one-trial non-matching-to-sample learning task to study 'recognition memory'. Nat Protoc 1:1306-1311.

Bieber M, Gronewold J, Scharf AC, Schuhmann MK, Langhauser F, Hopp S, Mencl S, Geuss E, Leinweber J, Guthmann J, Doeppner TR, Kleinschnitz C, Stoll G, Kraft P, Hermann DM (2019) Validity and reliability of neurological scores in mice exposed to middle cerebral artery occlusion. Stroke 50:2875-2882.

Blake JF, Burkard M, Chan J, Chen H, Chou KJ, Diaz D, Dudley DA, Gaudino JJ, Gould SE, Grina J, Hunsaker T, Liu L, Martinson M, Moreno D, Mueller L, Orr C, Pacheco P, Qin A, Rasor K, Ren L, et al. (2016) Discovery of (S)-1-(1-(4-chloro-3-fluorophenyl)-2-hydroxyethyl)-4-(2-((1-methyl-1H-pyrazol-5-yl)amino)pyrimidin-4-yl)pyridin-2(1H)-one (GDC-0994), an extracellular signal-regulated kinase 1/2 (ERK1/2) inhibitor in early clinical development. J Med Chem 59:5650-5660.

Boerckel JD, Chandrasekharan UM, Waitkus MS, Tillmaand EG, Bartlett R, Dicorleto PE (2014) Mitogen-activated protein kinase phosphatase-1 promotes neovascularization and angiogenic gene expression. Arterioscler Thromb Vasc Biol 34:1020-1031.

Bu F, Min JW, Munshi Y, Lai YJ, Qi L, Urayama A, McCullough LD, Li J (2019) Activation of endothelial ras-related C3 botulinum toxin substrate 1 (Rac1) improves post-stroke recovery and angiogenesis via activating Pak1 in mice. Exp Neurol 322:113059.

Bu F, Munshi Y, Furr JW, Min JW, Qi L, Patrizz A, Spahr ZR, Urayama A, Kofler JK, McCullough LD, Li J (2021) Activation of neuronal Ras-related C3 botulinum toxin substrate 1 (Rac1) improves post-stroke recovery and axonal plasticity in mice. J Neurochem 157:1366-1376.

Cao BQ, Tan F, Zhan J, Lai PH (2021) Mechanism underlying treatment of ischemic stroke using acupuncture: transmission and regulation. Neural Regen Res 16:944-954.

Collins LM, Downer EJ, Toulouse A, Nolan YM (2015) Mitogen-activated protein kinase phosphatase (MKP)-1 in nervous system development and disease. Mol Neurobiol 51:1158-1167.

Daneman R (2012) The blood-brain barrier in health and disease. Ann Neurol 72:648-672.

Deng LD, Qi L, Suo Q, Wu SJ, Mamtilahun M, Shi RB, Liu Z, Sun JF, Tang YH, Zhang ZJ, Yang GY, Wang JX (2022) Transcranial focused ultrasound stimulation reduces vasogenic edema after middle cerebral artery occlusion in mice. Neural Regen Res 17:2058-2063.

Ehrlich D, Pirchl M, Humpel C (2012) Effects of long-term moderate ethanol and cholesterol on cognition, cholinergic neurons, inflammation, and vascular impairment in rats. Neuroscience 205:154-166.

Farooq A, Zhou MM (2004) Structure and regulation of MAPK phosphatases. Cell Signal 16:769-779.

Fujikawa K, Presman E, Isner JM, Varticovski L (1999) Expression of Tie1 and Tie2 proteins during reendothelialization in balloon-injured rat carotid artery. J Vasc Res 36:272-281.

González-Mariscal L, Tapia R, Chamorro D (2008) Crosstalk of tight junction components with signaling pathways. Biochim Biophys Acta 1778:729-756.

Horita H, Wada K, Rivas MV, Hara E, Jarvis ED (2010) The dusp1 immediate early gene is regulated by natural stimuli predominantly in sensory input neurons. J Comp Neurol 518:2873-2901.

Jayaraj RL, Azimullah S, Beiram R, Jalal FY, Rosenberg GA (2019) Neuroinflammation: friend and foe for ischemic stroke. J Neuroinflammation 16:142.

Jiang X, Andjelkovic AV, Zhu L, Yang T, Bennett MVL, Chen J, Keep RF, Shi Y (2018) Blood-brain barrier dysfunction and recovery after ischemic stroke. Prog Neurobiol 163-164:144-171.

Kim E, Cho S (2021) CNS and peripheral immunity in cerebral ischemia: partition and interaction. Exp Neurol 335:113508.

Kimura S, Harashima H (2022) Non-invasive gene delivery across the blood-brain barrier: present and future perspectives. Neural Regen Res 17:785-787.

Kinney CM, Chandrasekharan UM, Mavrakis L, DiCorleto PE (2008) VEGF and thrombin induce MKP-1 through distinct signaling pathways: role for MKP-1 in endothelial cell migration. Am J Physiol Cell Physiol 294:C241-250.

Korotchenko VN, Saydmohammed M, Vollmer LL, Bakan A, Sheetz K, Debiec KT, Greene KA, Agliori CS, Bahar I, Day BW, Vogt A, Tsang M (2014) In vivo structure-activity relationship studies support allosteric targeting of a dual specificity phosphatase. ChemBioChem 15:1436-1445.

Liu L, Doran S, Xu Y, Manwani B, Ritzel R, Benashski S, McCullough L, Li J (2014) Inhibition of mitogen-activated protein kinase phosphatase-1 (MKP-1) increases experimental stroke injury. Exp Neurol 261:404-411.

Liu L, Yuan H, Yi Y, Koellhoffer EC, Munshi Y, Bu F, Zhang Y, Zhang Z, McCullough LD, Li J (2018) Ras-related C3 botulinum toxin substrate 1 promotes axonal regeneration after stroke in mice. Transl Stroke Res 9:506-514.

Maddahi A, Povlsen GK, Edvinsson L (2012) Regulation of enhanced cerebrovascular expression of proinflammatory mediators in experimental subarachnoid hemorrhage via the mitogen-activated protein kinase kinase/extracellular signal-regulated kinase pathway. J Neuroinflammation 9:274.

Manwani B, Liu F, Scranton V, Hammond MD, Sansing LH, McCullough LD (2013) Differential effects of aging and sex on stroke induced inflammation across the lifespan. Exp Neurol 249:120-131.

Min JW, Bu F, Qi L, Munshi Y, Kim GS, Marrelli SP, McCullough LD, Li J (2019) Inhibition of calcium/calmodulin-dependent protein kinase kinase β is detrimental in hypoxia-ischemia neonatal brain injury. Int J Mol Sci 20:2063.

Murphy LO, Blenis J (2006) MAPK signal specificity: the right place at the right time. Trends Biochem Sci 31:268-275.

Narasimhan P, Liu J, Song YS, Massengale JL, Chan PH (2009) VEGF stimulates the ERK 1/2 signaling pathway and apoptosis in cerebral endothelial cells after ischemic conditions. Stroke 40:1467-1473.

Paradis A, Leblanc D, Dumais N (2016) Optimization of an in vitro human blood-brain barrier model: Application to blood monocyte transmigration assays. MethodsX 3:25-34.

Parker BL, Larsen MR, Edvinsson LI, Povlsen GK (2013) Signal transduction in cerebral arteries after subarachnoid hemorrhage-a phosphoproteomic approach. J Cereb Blood Flow Metab 33:1259-1269.

Porter AG, Jänicke RU (1999) Emerging roles of caspase-3 in apoptosis. Cell Death Differ 6:99-104.

Qing CU, Zhang J, Wu S, Ling Z, Wang S, Li H, Li H (2014) Clinical classification and treatment of cubital tunnel syndrome. Exp Ther Med 8:1365-1370.

Robertson RT, Levine ST, Haynes SM, Gutierrez P, Baratta JL, Tan Z, Longmuir KJ (2015) Use of labeled tomato lectin for imaging vasculature structures. Histochem Cell Biol 143:225-234.

Rodrigues SF, Granger DN (2015) Blood cells and endothelial barrier function. Tissue Barriers 3:e978720.

Roux PP, Blenis J (2004) ERK and p38 MAPK-activated protein kinases: a family of protein kinases with diverse biological functions. Microbiol Mol Biol Rev 68:320-344.

Ruan J, Yao Y (2020) Behavioral tests in rodent models of stroke. Brain Hemorrhages 1:171-184.

Sawe N, Steinberg G, Zhao H (2008) Dual roles of the MAPK/ERK1/2 cell signaling pathway after stroke. J Neurosci Res 86:1659-1669.

Shi Y, Jiang X, Zhang L, Pu H, Hu X, Zhang W, Cai W, Gao Y, Leak RK, Keep RF, Bennett MV, Chen J (2017) Endothelium-targeted overexpression of heat shock protein 27 ameliorates blood-brain barrier disruption after ischemic brain injury. Proc Natl Acad Sci U S A 114:E1243-E1252.

Shi Y, Zhang L, Pu H, Mao L, Hu X, Jiang X, Xu N, Stetler RA, Zhang F, Liu X, Leak RK, Keep RF, Ji X, Chen J (2016) Rapid endothelial cytoskeletal reorganization enables early blood-brain barrier disruption and long-term ischaemic reperfusion brain injury. Nat Commun 7:10523.

Shin JA, Kim YA, Jeong SI, Lee KE, Kim HS, Park EM (2015) Extracellular signal-regulated kinase1/2-dependent changes in tight junctions after ischemic preconditioning contributes to tolerance induction after ischemic stroke. Brain Struct Funct 220:13-26.

Sun J, Nan G (2016) The mitogen-activated protein kinase (MAPK) signaling pathway as a discovery target in stroke. J Mol Neurosci 59:90-98.

Vincent T, Neve EP, Johnson JR, Kukalev A, Rojo F, Albanell J, Pietras K, Virtanen I, Philipson L, Leopold PL, Crystal RG, de Herreros AG, Moustakas A, Pettersson RF, Fuxe J (2009) A SNAIL1-SMAD3/4 transcriptional repressor complex promotes TGF-beta mediated epithelial-mesenchymal transition. Nat Cell Biol 11:943-950.

Yin KJ, Deng Z, Hamblin M, Xiang Y, Huang H, Zhang J, Jiang X, Wang Y, Chen YE (2010) Peroxisome proliferator-activated receptor delta regulation of miR-15a in ischemia-induced cerebral vascular endothelial injury. J Neurosci 30:6398-6408.

Zakkar M, Chaudhury H, Sandvik G, Enesa K, Luong le A, Cuhlmann S, Mason JC, Krams R, Clark AR, Haskard DO, Evans PC (2008) Increased endothelial mitogen-activated protein kinase phosphatase-1 expression suppresses proinflammatory activation at sites that are resistant to atherosclerosis. Circ Res 103:726-732.

Zhang T, Fang S, Wan C, Kong Q, Wang G, Wang S, Zhang H, Zou H, Sun B, Sun W, Zhang Y, Mu L, Wang J, Wang J, Zhang H, Wang D, Li H (2015) Excess salt exacerbates blood-brain barrier disruption via a p38/MAPK/SGK1-dependent pathway in permanent cerebral ischemia. Sci Rep 5:16548.

Zhang Y, Li X, Qiao S, Yang D, Li Z, Xu J, Li W, Su L, Liu W (2021) Occludin degradation makes brain microvascular endothelial cells more vulnerable to reperfusion injury in vitro. J Neurochem 156:352-366.

Zhuang S, Yan Y, Daubert RA, Han J, Schnellmann RG (2007) ERK promotes hydrogen peroxide-induced apoptosis through caspase-3 activation and inhibition of Akt in renal epithelial cells. Am J Physiol Renal Physiol 292:F440-447.

Zille M, Ikhsan M, Jiang Y, Lampe J, Wenzel J, Schwaninger M (2019) The impact of endothelial cell death in the brain and its role after stroke: A systematic review. Cell Stress 3:330-347.

Zong X, Li Y, Liu C, Qi W, Han D, Tucker L, Dong Y, Hu S, Yan X, Zhang Q (2020) Theta-burst transcranial magnetic stimulation promotes stroke recovery by vascular protection and neovascularization. Theranostics 10:12090-12110.

P-Reviewer: Rossignol J; C-Editor: Zhao M; S-Editors: Yu J, Li CH; L-Editors: Crow E, Song LP; T-Editor: Jia Y